

# Lattice QCD Calculation of Hadron Scattering Lengths \*

Y. Kuramashi <sup>a</sup>, M. Fukugita <sup>b</sup>, H. Mino <sup>c</sup>, M. Okawa<sup>a</sup> and A. Ukawa <sup>d</sup>,

<sup>a</sup> National Laboratory for High Energy Physics(KEK), Ibaraki 305, Japan

<sup>b</sup> Yukawa Institute for Theoretical Physics, Kyoto University, Kyoto 606, Japan

<sup>c</sup> Faculty of Engineering, Yamanashi University, Kofu 400, Japan

<sup>d</sup> Institute of Physics, University of Tsukuba, Ibaraki 305, Japan

Method of calculating hadron multi-point functions and disconnected quark loop contributions which are not readily accessible through conventional techniques is proposed. Results are reported for  $\pi\pi$ ,  $\pi N$  and  $N N$  scattering lengths and the flavor singlet-non singlet meson mass splitting estimated in quenched QCD.

## 1. Introduction

Numerical simulation of lattice QCD has been applied to an increasingly larger variety of strong interaction observables over the years. Yet these quantities all share the feature that their calculation can be reduced to that of connected hadron 2-point functions. A number of physically interesting quantities do not fall into this class: scattering amplitudes requiring hadron 4-point functions are a prime example. Amplitudes involving disconnected quark loops such as the flavor singlet meson propagator and  $\pi N$  sigma term represent another important example. Technically the difficulty stems from the fact that calculation of these amplitudes requires quark propagators connecting arbitrary pairs of space-time sites. With the conventional method of point source the necessary number of quark matrix inversions equals the space-time lattice volume, which would require a prohibitively large amount of computer time.

We found that the wall source technique[1,2], in particular *without gauge fixing* as were employed in the original proposals of extended sources[1], could be effectively used to overcome the problem with a modest cost of computing power[3]. The method has been applied to calculate the full  $\pi\pi$ ,  $\pi N$  and  $N N$  4-point functions at vanishing relative momentum, from which we extracted the

$s$ -wave scattering lengths with the help of the relation between the two-particle energy in a finite box and the scattering length[4,5]. With a slight extension the method also allows an efficient calculation of the two quark loop contribution to the flavor singlet  $\eta'$  propagator.

In this report we present the results together with some details of the technique. All of the simulations have been made within quenched QCD at  $\beta = 5.7$  mostly employing the lattice size of  $12^3 \times 20$ .

## 2. Calculational technique

Consider the box diagram contributing to  $\pi\pi$  scattering with zero-momentum projected pion operators placed at the four time slices  $t_i (i = 1, \dots, 4)$ . To evaluate this amplitude on an  $L^3 \times T$  lattice, we calculate  $T$  quark propagators  $G_t(n)$  with a wall source placed at the time slice  $t = 1, \dots, T$ . With these propagators we form

$$\sum_{\vec{x}_2, \vec{x}_3} \langle \text{Tr}(G_{t_1}^\dagger(\vec{x}_2, t_2) G_{t_4}(\vec{x}_2, t_2) G_{t_4}^\dagger(\vec{x}_3, t_3) G_{t_1}(\vec{x}_3, t_3)) \rangle, \quad (1)$$

which equals the box amplitude except that the pion operators at the time slices  $t_1$  and  $t_4$  have to be taken to be non-local in space without insertion of gauge link factors.

Fixing gauge configurations to some gauge is usually employed to deal with the non-locality[2].

\*presented by Y. Kuramashi

A problem with this method is that excited states such as  $\rho$  may contaminate signals for small time intervals. Alternatively one may take the gauge field average *without gauge fixing* since gauge variant noise should cancel out in the average. One might worry that the noise overwhelms the signal in practice since for each time slice  $t_1$  and  $t_4$  there are  $O((L^3)^2)$  gauge dependent non-local terms relative to  $O(L^3)$  local gauge invariant ones. It is our experience, however, that the noise level is controllably low at least for the pion.

Calculating  $T$  quark propagators has another advantage. For two hadron operators placed at the same time slice, as is necessary if only the quark propagator for a wall source at  $t = 0$  is available, color Fierz rearrangement of quark lines takes place. This leads to a mixing among amplitudes having different quark line topologies, which is numerically not straightforward to disentangle[6]. Such a complication can be trivially avoided with the present method by placing hadron operators at different time slices.

The present method can apply not only to a calculation of 4-point functions, but also to more general class of evaluation of  $n$ -point functions of hadrons.

### 3. $\pi\pi$ scattering lengths

We have applied our method to calculate the  $I = 0$  and  $2$   $\pi\pi$  scattering lengths for both Kogut-Susskind and Wilson quark actions, of which the Kogut-Susskind result has already been published[3]. The procedure leading from  $\pi\pi$  4-point functions to scattering lengths is as follows. The energy shift of the two-pion state  $\delta E = E - 2m_\pi$  is extracted from the ratio of 4- to 2-point functions,

$$\begin{aligned} R(t) &= \frac{<\pi(t+1)\pi(t)\pi(1)\pi(0)>}{<\pi(t)\pi(0)><\pi(t+1)\pi(1)>} \\ &= Z \exp(-\delta Et). \end{aligned} \quad (2)$$

In practice we use a linear fit  $Z(1 - \delta Et)$  in our quenched simulation since  $O(t^2)$  terms are generally not correct in the absence of dynamical quark loops. The fitted values can then be converted to  $s$ -wave scattering length  $a_0$  using the Lüscher's

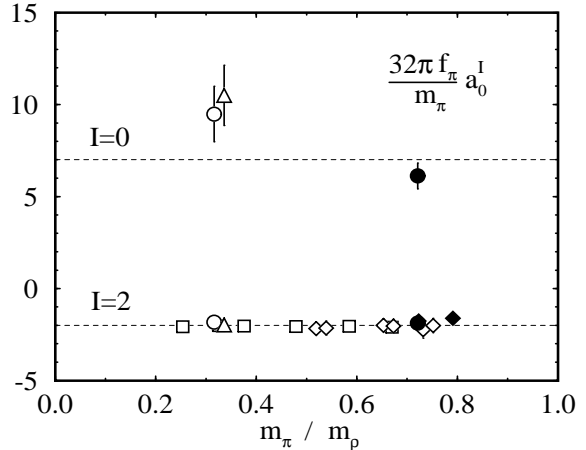


Figure 1.  $I = 0$  and  $2$   $s$ -wave  $\pi\pi$  scattering lengths  $a_0^I$ . Filled and open symbols denote Wilson and Kogut-Susskind results. Triangles are for Coulomb gauge fixing. Squares ( $\beta = 5.7$ ) and diamonds ( $\beta = 6.0$ ) for  $I = 2$  are from Ref. [6]. Dotted lines indicate predictions of current algebra.

relation[5]:

$$E - 2m_\pi = -\frac{4\pi a_0}{m_\pi L^3} \left( 1 + c_1 \frac{a_0}{L} + c_2 \left( \frac{a_0}{L} \right)^2 \right) + O(L^{-6}) \quad (3)$$

with  $c_1 = -2.837297$ ,  $c_2 = 6.375183$ .

The two calculations respectively used 160 ( $m_q a = 0.01$ ; KS) and 70 ( $K = 0.164$ ; Wilson)  $12^3 \times 20$  configurations *without gauge fixing*. The  $I = 2$  amplitude has been studied in pioneering work[7,6]. The calculation for  $I = 0$  is more difficult since box and double annihilation diagrams with quarkless intermediate state, both requiring a full application of our method, contribute. We found that the double annihilation amplitude is very small, consistent with chiral perturbation theory and the OZI rule, and that the  $I = 0$  amplitude exhibits a clear signal for attraction.

Our results for the scattering lengths are summarized in Fig. 1 together with those of Ref. [6] for  $I = 2$ . Triangles are the results obtained with Coulomb gauge fixing described below. We use  $m_\pi$  and  $f_\pi$  measured on the same set of configurations, corrected by the improved  $Z$  factor[8] for  $f_\pi$  for the Wilson case ( $Z = 1$  for the KS case since the conserved current was employed). We observe an agreement of lattice results with cur-

rent algebra within 1–2 standard deviations for both  $I = 0$  and 2 channels. It is somewhat unexpected that the agreement persists up to a quite heavy quark with  $m_\pi/m_\rho \approx 0.7 - 0.8$ .

The errors shown in Fig. 1 are statistical only. For the Kogut-Susskind action the lack of degeneracy of pions in the Nambu-Goldstone and other channels invalidates the  $O(L^{-5})$  term in (3)[6]. This leads to an uncertainty of 10% in the  $I = 0$  result (that for the  $I = 2$  result is less than 1%). Another source of systematic error is violation of scaling due to a fairly large lattice spacing of our simulation ( $a \approx 0.2$  fm at  $\beta = 5.7$ ). The results of Ref. [6] obtained at  $\beta = 5.7$  and 6.0 suggest, however, that this effect may be small, at least for  $I = 2$ .

We have repeated the calculation with Coulomb gauge fixing employing 60 gauge configurations, and found the results for  $R(t)$  to be completely consistent with those obtained without gauge fixing on the same set of configurations. Comparing the two results, we found that the magnitude of errors is larger for the non-gauge fixed case. The amount of increase of errors, however, is contained at the level of a factor of 1.5–2 times those for the Coulomb gauge fixing, showing that gauge variant noise does not give rise to a serious problem for calculation of  $\pi\pi$  4-point functions. The results for scattering length obtained with Coulomb gauge fixing are plotted in Fig. 1.

All the results in Fig. 1 are obtained in quenched simulations, and hence do not include effects of dynamical quarks. A potential problem with the quenched calculation is that it could be affected by infrared singularities due to  $\eta'$  loops suggested recently[9]. Since the appearance of such singularities is a general issue in quenched QCD, we shall discuss it in the subsequent section, in connection with the  $U(1)$  problem. The problem of this unphysical singularity anyway does not arise if calculations are made on full QCD gauge configurations[10], which is a straightforward task to be carried out.

#### 4. $\eta'$ meson mass in quenched QCD

The problem of a large mass splitting between the flavor singlet  $\eta'$  and the pion octet is known

as the  $U(1)$  problem. In the large  $N_c$  expansion the mass splitting  $m_0^2 = m_{\eta'}^2 - m_\pi^2$  arises from iteration of virtual quark loops in the  $\eta'$  propagator, each loop giving a factor  $m_0^2/(p^2 + m_\pi^2)$ . In quenched QCD the series terminates at two quark loops. This implies that the magnitude of  $m_0$  may be estimated through a comparison of the two quark loop amplitude having a double pole  $m_0^2/(p^2 + m_\pi^2)^2$  with the one quark loop amplitude with a single pole  $1/(p^2 + m_\pi^2)$ ; the ratio of the two amplitudes, each projected onto zero spatial momentum, is expected to behave as

$$R(t) = \frac{\langle \eta'(t)\eta'(0) \rangle_{\text{2-loop}}}{\langle \eta'(t)\eta'(0) \rangle_{\text{1-loop}}} \approx \frac{m_0^2}{2m_\pi} t. \quad (4)$$

It has been suggested that the double pole in the  $\eta'$  propagator with a mass degenerate with that of  $\pi$  leads to infrared divergences which are not suppressed by powers of the pion mass toward the chiral limit in quenched QCD[9]. To one-loop order in chiral perturbation theory, for instance, the pion mass receives a correction of the form,

$$(m_\pi^{\text{1-loop}})^2 = m_\pi^2 \left( 1 - \frac{m_0^2}{8N_f\pi^2 f_\pi^2} \ln \frac{m_\pi}{\Lambda} \right). \quad (5)$$

The problem for  $\pi\pi$  scattering could be even more serious[11]. The double annihilation diagram with two quark loops can be deformed into an  $\eta'$  loop diagram with two insertions of the  $m_0^2$  vertex. Calculating the diagram in chiral perturbation theory, one finds a divergent imaginary part at threshold in the  $s$  channel, and in the  $t$  channel a contribution of the form,

$$\delta E = \frac{1}{384\pi^2} \frac{m_0^4}{N_f^2 m_\pi^2 f_\pi^4} \frac{1}{L^3} \quad (6)$$

to the energy shift of the two pion system, which diverges quadratically as  $m_\pi \rightarrow 0$ . Whether such terms affect results of quenched simulations depends on the magnitude of  $m_0$ . A direct quenched estimate of  $m_0$  through (4) is also important in this respect.

The two quark loop amplitude needed in (4) can be evaluated by the technique discussed above. We solve for the quark propagator with unit source *at every space-time site without gauge fixing*. (Note that this is crucial for the present

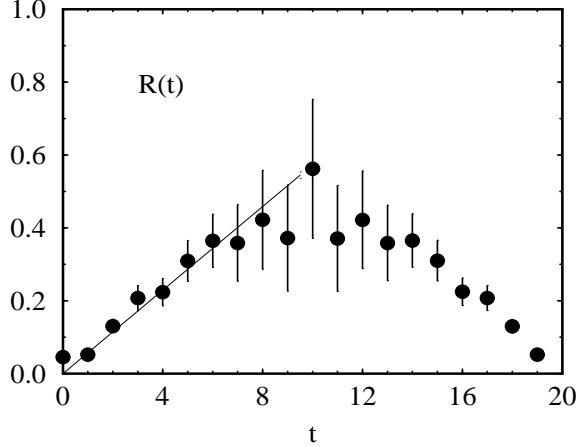


Figure 2. Ratio of two- and one-quark loop contribution to the  $\eta'$  propagator at  $K = 0.1665$  and  $\beta = 5.7$  on a  $12^3 \times 20$  lattice.

case.) With this quark propagator  $G(\vec{n}, t) \equiv \sum_{(\vec{n}'', t'')} G(\vec{n}, t; \vec{n}'', t'')$  we form the expression,

$$\sum_{\vec{n}, \vec{n}'} \text{Tr}\{G(\vec{n}, 0)\gamma_5\} \text{Tr}\{G^\dagger(\vec{n}', t)\gamma_5\}. \quad (7)$$

This equals the two quark amplitude projected onto zero spatial momentum up to gauge-variant non-local terms which, however, cancel out in the ensemble average. A very nice feature of this technique is that it requires only a single quark matrix inversion for each gauge configuration.

In Fig. 2 we plot the result for the ratio given in (4) for Wilson quark action obtained with 160 configurations at  $K = 0.1665$ . We observe a quite clear signal for a linear increase in  $t$ . We then extract the  $m_0$  parameter by a fit of form (4) over the range  $4 \leq t \leq 8$ . The results at two values of  $K$  together with a linear extrapolation in  $1/K$  to  $K_c = 0.1694$  are shown in Fig. 3 where conversion to physical units is made with  $a^{-1} = 1.45(2)$  GeV determined from the  $\rho$  meson mass. We refer to earlier attempts[12,13] that calculated the two quark loop amplitude. In particular the authors of Ref. [13] estimated  $m_0 = 530$  MeV at  $m_\pi/m_\rho = 0.71$  and  $330$  MeV at  $m_\pi/m_\rho = 0.34$  with  $a^{-1} = 1.81$  GeV from a calculation with the  $\eta'$  source and sink fixed at the spatial origin using 10 configurations generated with a non-standard gauge action on an  $8^3 \times 16$  lattice.

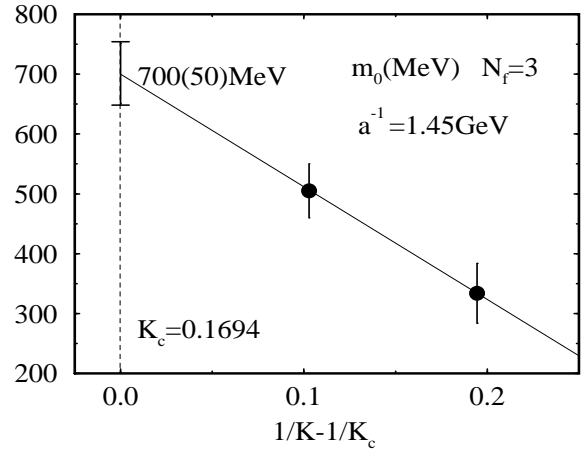


Figure 3.  $m_0$  in physical units as a function of  $1/K - 1/K_c$ .

Our value  $m_0 = 700(50)$  MeV at  $K_c$  may be compared to the ‘experimental’ value of 850 MeV deduced from the Witten-Veneziano formula[14]. Another comparison, more directly based on lattice QCD, is to invoke the original  $U(1)$  Ward identity relation  $m_0^2 = 6\chi/f_\pi^2$  with  $\chi$  the topological susceptibility. Using  $\chi = 4.28(33) \times 10^{-4}$  and  $f_\pi = 0.0616(40)$  at  $K_c$  we obtained on the same set of configurations as for  $m_0$ , we find  $m_0 = 1190(90)$  MeV.

Let us now consider the question of infrared singular terms induced by  $\eta'$  loops in quenched QCD. With our result for  $m_0$  and  $f_\pi$ , we find that the coefficient of the logarithmic correction for the pion mass in (5) equals 0.076 at  $m_\pi/m_\rho = 0.61$  ( $K = 0.1665$ ). Quenched pion mass data presently restricted to  $m_\pi/m_\rho \gtrsim 0.5$  do not show evidence of the logarithm with such a small coefficient[15]. The magnitude of (6) contributing to the  $\pi$ - $\pi$  scattering length is even smaller. For our Kogut-Susskind simulation, taking the Wilson result  $m_0a = 0.48$  at  $K_c$  as an indicative value and using measured  $m_\pi$  and  $f_\pi$  we find  $\delta E = 3.4 \times 10^{-5}$  at  $m_\pi/m_\rho = 0.32$ , which may be compared with the value  $\delta E = 1.2(4.0) \times 10^{-4}$  extracted from the slope of the double annihilation diagram. We conclude that the possible failure of the quenched approximation due to  $\eta'$  loops does not become manifest unless the simulation is made with a quark mass much smaller than the

value being taken in the current study.

### 5. $\pi$ - $N$ scattering lengths

The wall source technique without gauge fixing does not yield good signals for the nucleon. We therefore used the Coulomb gauge fixing at the  $t = 0$  time slice for the nucleon source to calculate  $\pi$ - $N$  4-point functions. In Fig. 4 we show our preliminary result for the ratio  $R^I(t)$  of  $\pi$ - $N$  amplitude divided by the propagators of  $\pi$  and  $N$  obtained with 30 configurations with the Wilson quark action at  $K = 0.164$ . We observe a good signal for  $I = 3/2$ . The data is much worse for  $I = 1/2$ , marginally indicative of a positive slope (*i.e.*, attraction) expected from the experiment. Extracting the energy shift by a linear fit in  $t$  over the interval  $4 \leq t \leq 8$ , we find for the scattering lengths

$$a_0^{I=3/2} \cdot \frac{8\pi f_\pi^2}{\mu_{\pi N}} = -0.95(13) \quad [-1] \quad (8)$$

$$a_0^{I=1/2} \cdot \frac{8\pi f_\pi^2}{\mu_{\pi N}} = +1.6(0.7) \quad [+2] \quad (9)$$

where  $\mu_{\pi N} = m_\pi m_N / (m_\pi + m_N)$  and numbers in square brackets are prediction of current algebra. Despite a heavy quark mass ( $m_\pi/m_\rho = 0.73$  at  $K = 0.164$ ) our results are consistent with current algebra both for  $I = 1/2$  and  $I = 3/2$  channels. The error is large for  $I = 1/2$ , however.

Clearly reducing the error is much desired for  $I = 1/2$ . It is also interesting to repeat the calculation for smaller quark masses. However, both of these extensions are not easy in practice. A simple argument suggests that the errors of  $R(t)$  grow exponentially  $\delta R(t) \propto e^{\alpha t}$  with  $\alpha = m_N - 3/2m_\pi$  or  $m_N - 1/2m_\pi$  depending on the topology of quark lines[16]. Our numerical data indeed exhibits such dependence with the expected slope. This means that a reduction of errors at large values of  $t$  requires a substantial increase of statistics. The situation appears worse for lighter quarks since  $m_N$  remains non-zero while  $m_\pi$  becomes smaller, leading to a larger value for the slope  $\alpha$ . The only way to reduce errors would be to increase  $\beta$  with a simultaneous enlargement of the lattice size. In this regard the  $\pi$ - $N$  case turns out to be more difficult in nature

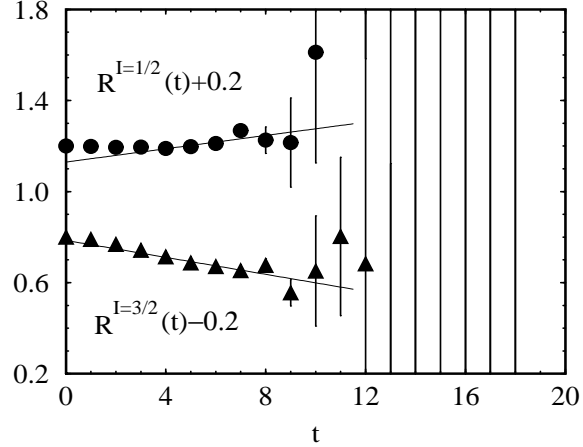


Figure 4.  $\pi$ - $N$  amplitudes for  $I = 1/2$  and  $3/2$ . Data are shifted by  $\pm 0.2$  to avoid overlap.

than the  $\pi$ - $\pi$  case; for the latter the errors grow only modestly as  $\delta R(t) \propto e^{2m_\pi t}$  even for the worst case of the double annihilation diagram[3] whose slope becomes smaller toward the chiral limit.

### 6. $N$ - $N$ scattering lengths

The  $N$ - $N$  scattering lengths are experimentally known to be very large[17];

$$a_0(^1S_0) = +20.1(4) \text{ fm}, \quad (10)$$

$$a_0(^3S_1) = -5.432(5) \text{ fm}. \quad (11)$$

As opposed to the  $\pi$ - $\pi$  and  $\pi$ - $N$  cases, the  $N$ - $N$  amplitudes are not constrained by chiral symmetry. The large values above are, therefore, a purely dynamical phenomenon whose successful derivation is a challenge posed to lattice QCD.

We note that the negative sign in the  $^3S_1$  channel is due to the presence of the deuteron bound state (Levinson's theorem). This brings in an additional complication in an attempt at a realistic calculation of the scattering lengths, since the energy of the lowest scattering state orthogonal to the bound-state deuteron has to be computed to apply Lüscher's relation to give the correct scattering lengths.

Here we report on a less ambitious study employing quite a heavy Wilson quark with  $m_\pi/m_\rho = 0.86$  ( $K = 0.16$ ). For such a heavy

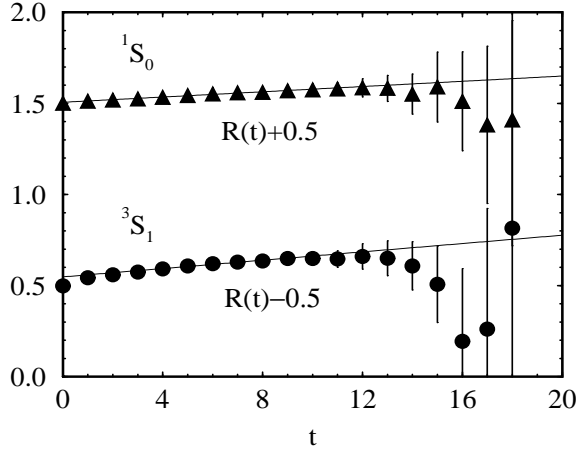


Figure 5.  $N$ - $N$  amplitudes for  $^3S_1$  and  $^1S_0$  channels. Data are shifted by  $\pm 0.5$  to avoid overlap.

quark we may expect the deuteron to become unbound since the range of pion exchange is reduced. In this case the scattering lengths for both  $^3S_1$  and  $^1S_0$  channels can be extracted from the lowest  $N$ - $N$  energy, and we expect both to be positive in sign and large.

Anticipating a large scattering length we have made simulations on a  $20^4$  lattice with Wilson quark action using 30 gauge configurations with Coulomb gauge fixing. The result for the ratio  $R(t)$  is shown in Fig. 5. The positive slope corresponding to a negative energy shift for both channels is consistent with our expectation above. Numerically, we find

$$a_0(^1S_0) = 1.0(3) \text{ fm}, \quad (12)$$

$$a_0(^3S_1) = 1.2(2) \text{ fm}. \quad (13)$$

for the scattering length in physical units using  $a^{-1} = 1.45$  GeV. Although these values are much smaller than the experimental values they are about a factor 3 – 4 larger than  $\pi$ - $\pi$  and  $\pi$ - $N$  scattering lengths at similar quark masses, *e.g.*,  $a^{I=0}(\pi\text{-}\pi) = 0.421(23)$  fm and  $a^{I=1/2}(\pi\text{-}N) = 0.30(14)$  fm at  $K = 0.164$ .

We consider that the present result is encouraging; the most interesting problem left with us is to examine whether these scattering lengths increase rapidly as the quarks mass is reduced.

## REFERENCES

1. R. D. Kenway, in *Proc. XXII Int. Conf. on High Energy Physics*, eds. A. Meyer and E. Wieczorek, vol.1, p.51 (Leipzig, 1984); A. Billoire, E. Marinari and G. Parisi, *Phys. Lett.* 162B (1985) 160.
2. G. W. Kilcup, *Lattice 89*, *Nucl. Phys. B (Proc. Suppl.)* 17 (1990) 533; R. Gupta *et al.*, *Phys. Rev. D43* (1991) 2003.
3. Y. Kuramashi, M. Fukugita, H. Mino, M. Okawa and A. Ukawa, *Phys. Rev. Lett.* 71 (1993) 2387.
4. H. Hamber, E. Marinari, G. Parisi and C. Rebbi, *Nucl. Phys. B225[FS9]* (1983) 475.
5. M. Lüscher, *Commun. Math. Phys.* 104 (1986) 177; 105 (1986) 153; *Nucl. Phys. B354* (1991) 531.
6. S. R. Sharpe, R. Gupta and G. W. Kilcup, *Nucl. Phys. B383* (1992) 309; R. Gupta, A. Patel and S. R. Sharpe, *Phys. Rev. D48* (1993) 388.
7. M. Guagnelli, E. Marinari and G. Parisi, *Phys. Lett.* 240B (1990) 188.
8. G. P. Lepage and P. Mackenzie, *Phys. Rev. D48* (1993) 2250.
9. C. Bernard and M. Golterman, *Phys. Rev. D46* (1992) 853; preprint WASH-HEP-93-32 (1993); S. R. Sharpe, *Phys. Rev. D46* (1992) 3146; J. Labrenz, in these proceedings.
10. M. Fukugita, N. Ishizuka, H. Mino, M. Okawa and A. Ukawa, *Phys. Rev. D47* (1993) 4739.
11. C. Bernard, M. Golterman, J. Labrenz, S. Sharpe and A. Ukawa, in these proceedings.
12. M. Fukugita, T. Kaneko and A. Ukawa, *Phys. Lett.* 145B (1984) 93.
13. S. Itoh, Y. Iwasaki and T. Yoshié, *Phys. Rev. D36* (1987) 527.
14. E. Witten, *Nucl. Phys. B156* (1979) 269; G. Veneziano, *Nucl. Phys. B159* (1979) 213.
15. S. R. Sharpe, *Lattice 92*, *Nucl. Phys. B(Proc. Suppl.)* 30 (1993) 213; A. Ukawa, *ibid.*, 3.
16. G. P. Lepage in *Proc. of TASI'89 Summer School*, eds. T. DeGrand and D. Toussaint (World Scientific, Singapore, 1990) p.97.
17. See, *e.g.*, G. A. Miller *et al.*, *Phys. Rep.* 194 (1990) 1.

This figure "fig1-1.png" is available in "png" format from:

<http://arxiv.org/ps/hep-lat/9312016v1>

This figure "fig1-2.png" is available in "png" format from:

<http://arxiv.org/ps/hep-lat/9312016v1>

This figure "fig1-3.png" is available in "png" format from:

<http://arxiv.org/ps/hep-lat/9312016v1>

This figure "fig1-4.png" is available in "png" format from:

<http://arxiv.org/ps/hep-lat/9312016v1>

This figure "fig1-5.png" is available in "png" format from:

<http://arxiv.org/ps/hep-lat/9312016v1>